Electromagnetic Modeling of Ferrites Using Shell Elements and Random Grain Structures

Paavo Rasilo[1], Joonas Vesa[1], and Johan Gyselinck[2]

[1] Unit of Electrical Engineering, Tampere University, 33720 Tampere, Finland, paavo.rasilo@tuni.fi
[2]BEAMS Department, Université libre de Bruxelles, 1050 Brussels, Belgium

We present a novel approach for stochastic finite element (FE) modeling of electromagnetic fields in ferrites, combining a thin shell model (TSM) for highly permittive grain boundaries with a Voronoi-tessellation-based geometry generation algorithm. The TSM is validated in the case of a periodic grain structure in a linear 2-D time-harmonic case over a frequency range of 10 kHz – 1 GHz, and problems related to standard FE discretization are discussed. The TSM is then applied in a stochastic study for simulating the effect of varying grain structure on the effective resistivity, losses and reactive power densities of a ferrite core.

***Index Terms*—Eddy currents, ferrites, finite element analysis, random media.**

I. Introduction

SOFT FERRITES are commonly used for magnetic cores of power-electronic inductors. Despite their long-standing use, there is no consensus on their exact power loss mechanisms, in particular at high frequencies. The losses consist of quasi-static hysteresis losses as well as dynamic losses which are typically associated with both eddy currents and spin damping [1]. Dielectric losses and the resonant- or relaxation-type characteristics of the magnetization processes are also discussed in the literature [2].

The problem of estimating of ferrite losses is further complicated by their random grain structure. Stochastic analysis with realistic grain structures would be required in order to analyze the losses. However, sintered ferrites consist of grains sized 10 to 100 μm and separated by highly resistive and permittive boundaries with thicknesses in the range of 1 nm [1]. Accurate finite element (FE) discretization of such a multiscale problem would lead to prohibitively large systems of equations or bad-quality elements, such as the triangles shown in Fig. 1 (a), whose corner angles grow towards 180° when the boundary thickness d decreases, resulting in inaccurate description of derivatives [3]. So far the modeling attempts have been based on lumped parameter models [4]-[6] or simplified deterministic and periodic grain structures [1], [7], [8] with non-realistic exaggerated dimensions to avoid discretizing the thin boundaries. It has not been studied, how well the electromagnetic properties of ferrites can be captured by such periodic geometries, and how much they might vary due to variations in the geometry. Although some attempts have been taken to imitate the random geometries of soft magnetic composites [9], similar approaches for ferrites seem to be missing.

This paper has two goals. First, we will develop a thin shell model (TSM) for the boundary layers so that the discretization problem related to thin layers is avoided. The TSM follows the idea of [10] and is validated by comparison against finely-discretized geometries with unstructured and structured meshes in the case of a periodic grain structure. Secondly, we will develop a Voronoi-tessellation-based algorithm for generating geometries with random grain structures with a fixed average grain size. The stochastic properties of eddy-current losses and capacitive power densities in ferrites are then studied and compared to the periodic structures.

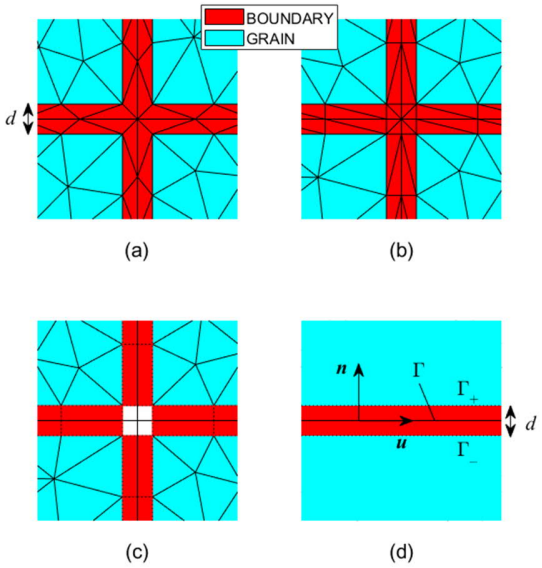

Fig. 1. Examples of (a) unstructured and (b) structured meshes, as well as (c) virtual discretization and (d) local coordinate system used for ferrite boundaries.

II. Methods

A. Problem setting and formulations

Time-harmonic 2-D formulations are considered for both electrodynamic (ED) and electro-magnetodynamic (EMD) problems. In both settings, the electric field strength $\boldsymbol{E}$, electric current density $\boldsymbol{J} = \sigma\boldsymbol{E}$, and electric flux density $\boldsymbol{D} = \varepsilon\boldsymbol{E}$ are parallel to the xy-plane. The magnetic field strength $\boldsymbol{H} = H\boldsymbol{z}$ and flux density $\boldsymbol{B} = B\boldsymbol{z} = \mu H\boldsymbol{z}$ point perpendicularly to the plane and can be handled as scalars H and B. All quantities are handled as peak-valued complex phasors. Since the small-signal behavior of the materials is studied over a wide frequency range, linear material properties are assumed, so that the electrical conductivity σ, permittivity ε and permeability μ are independent of the field quantities. The considered calculation domains Ω are squares with side lengths L. The sides parallel to

the x-axis are denoted Γ_{top}, Γ_{bottom} and the sides parallel to the y-axis Γ_{left}, Γ_{right}. The calculation domains are divided into $m = k^2$ grains (k being an integer) with either a deterministic arrangement into $k \times k$ equally sized squares or a random arrangement with variable grain sizes. The grain and boundary dimensions and material parameter values are adopted from [6] with the exception that constant permittivity values are used instead of frequency dependent ones. The material parameter values are given in Table I.

TABLE I
CONSIDERED MATERIAL PARAMETERS AND DIMENSIONS

Parameter	Value
Grain conductivity σ	117.6 S/m
Grain permittivity ε	350 ε_0
Grain permeability μ	100 μ_0
Boundary conductivity σ	5.3 mS/m
Boundary permittivity ε	100 ε_0
Boundary permeability μ	μ_0
Average grain size s_{av}	17 μm
Boundary layer thickness d	20 nm

ε_0 and μ_0 denote the permittivity and permeability of free space.

The ED formulation corresponds to a typical resistivity measurement setup in which a sinusoidally alternating source voltage V is applied over a ferrite sample and the total current consisting of free charges and displacement current is measured. The problem is given by

$$-\nabla\cdot\left(\sigma+j\omega\varepsilon\right)\nabla v=0 \text{ with } v=\begin{cases}0 & \text{at } \Gamma_{\text{left}}\\ V & \text{at } \Gamma_{\text{right}}\end{cases} \tag{1}$$

where v is an electric scalar potential for which $\boldsymbol{E} = -\nabla v$, and $\omega = 2\pi f$ is the angular excitation frequency. We are interested in the effective resistivity

$$\rho_{\text{eff}}=\frac{\int_\Omega E_{\text{x}}\,d\Omega}{\int_\Omega\left(\sigma+j\omega\varepsilon\right)E_{\text{x}}\,d\Omega}=\frac{LV}{\int_\Omega\left(\sigma+j\omega\varepsilon\right)E_{\text{x}}\,d\Omega} \tag{2}$$

which is complex-valued and frequency dependent due to the permittive materials.

The EMD formulation corresponds to an excitation by a time-varying magnetic field and is given by

$$-\nabla\cdot\frac{1}{\sigma+j\omega\varepsilon}\nabla T+j\omega\mu\left(T+H_{\text{s}}\right)=0$$

$$\text{with } T=0 \text{ at } \cup\left(\Gamma_{\text{top}},\Gamma_{\text{bottom}},\Gamma_{\text{left}},\Gamma_{\text{right}}\right) \tag{3}$$

where T is the z-component of an electric vector potential $\boldsymbol{T} = T\boldsymbol{z}$ for which $\boldsymbol{J} + j\omega\boldsymbol{D} = \nabla \times \boldsymbol{T}$, and H_{s} is the source field imposed into the sample. In this case, we are interested in the eddy-current loss density p_{cl} as well as the rate-of-change of the magnetic (q_{ind}) and electric (q_{cap}) field energies averaged over the domain:

$$p_{\text{cl}}=\frac{1}{L^2}\int_\Omega\frac{1}{2}\sigma\left\|\boldsymbol{E}\right\|^2 d\Omega \tag{4a}$$

$$q_{\text{ind}}=\frac{1}{L^2}\int_\Omega\frac{1}{2}\omega\mu\left|H\right|^2 d\Omega \tag{4b}$$

$$q_{\text{cap}}=\frac{1}{L^2}\int_\Omega\frac{1}{2}\omega\varepsilon\left\|\boldsymbol{E}\right\|^2 d\Omega. \tag{4c}$$

The eddy currents are obviously neglected in the ED formulation. However, this formulation was chosen for calculating ρ_{eff}, since imposing the source voltage is more straightforward compared to the EDM formulation, where $\boldsymbol{E}$ is a non-conservative vector field. Both formulations have been chosen so that discretization with nodal elements is possible.

B. Standard finite element method

Standard Galerkin FE discretization of (1) and (3) with shape functions N_i and nodal values $\boldsymbol{v} = (v_1, v_2, \ldots)$ for v, $\boldsymbol{t} = (t_1, t_2, \ldots)$ for T and $\boldsymbol{h}_{\text{s}} = (H_{\text{s}}, H_{\text{s}}, \ldots)$ for (constant) H_{s} leads to

$$\boldsymbol{S}\boldsymbol{v}=\boldsymbol{0} \text{ and } \left(\boldsymbol{S}+j\omega\boldsymbol{T}\right)\boldsymbol{t}=-j\omega\boldsymbol{T}\boldsymbol{h}_{\text{s}}, \tag{5}$$

where

$$S_{ij}=\int_\Omega\left(\sigma+j\omega\varepsilon\right)^{\pm1}\left(\nabla N_i\right)\cdot\left(\nabla N_j\right)d\Omega \tag{6a}$$

$$T_{ij}=\int_\Omega\mu N_i N_j\,d\Omega \tag{6b}$$

are the stiffness and damping matrices. The exponent of the complex conductivity $\sigma + j\omega\varepsilon$ depends on formulation (1) or (3). This standard FE formulation is simple to implement. The most common practice is to use an unstructured mesh as shown in Fig. 1 (a). However, as shown in [3], elements with corner angles close to 180° typically lead to numerical errors in description of derivatives, while similar problems are avoided for right-angled elements shown in Fig. 1 (b). Right-angled elements can be rather easily generated for periodic geometries using structured meshes for the boundaries, but this will become difficult if random grain structures are to be studied.

C. Thin shell model

To avoid the discretization problems related to the boundary regions, a TSM is developed for solving (5) in the boundaries. We first virtually discretize the boundaries with rectangular elements whose edges are oriented perpendicularly to the boundaries, like shown in Fig. 1 (c). Virtual discretization means that the boundary elements and their coordinate mappings are not considered in the surface integrations (6). Instead, we assume the local coordinate system presented in Fig. 1 (d), describing the boundary layers as $\Gamma \times [0, d]$. The intersections of boundary lines shown by the white squares in Fig. 1 (c) remain undiscretized, but this is assumed to have a negligible effect on the field solutions.

After the virtual discretization, the FE matrices corresponding to the boundary layers can be written as

$$S_{ij}=\left(\sigma+j\omega\varepsilon\right)^{\pm1}\int_\Gamma\left[\int_0^d\left(\frac{\partial N_i}{\partial u}\frac{\partial N_j}{\partial u}+\frac{\partial N_i}{\partial n}\frac{\partial N_j}{\partial n}\right)dn\right]d\Gamma \tag{7a}$$

$$T_{ij} = \mu \int_{\Gamma} \left[\int_{0}^{d} N_i N_j \, dn \right] d\Gamma \,, \tag{7b}$$

in which the surface integrations are separated into integrations parallel and perpendicular to the boundaries. The perpendicular integrations in the square brackets are performed analytically, and thus only the boundary lines Γ need to be discretized in the FE model. Separate nodes and degrees of freedom for v and T are used at the two sides Γ_- and Γ_+. The TSM accounts for the displacement currents and, in the case of the EDM formulation, also the eddy currents in the boundaries.

D. Random geometries

Since the boundary surfaces do not need to be discretized, it becomes relatively easy to create random grain structures for stochastic studies using 2-D Voronoi tessellations, which is a popular technique for imitating polycrystalline microstructures in mechanics [11]. We first tessellate the xy-plane using a standard Voronoi tessellation with m randomly chosen seed points uniformly distributed in $(0,1) \times (0,1)$. The tessellation is then bound by the unit square $[0,1] \times [0,1]$. As a result, m randomly arranged regions with areas A_i, $i = 1, \ldots, m$ such that $\sum_{i=1}^{m} A_i = 1$ are obtained, representing the grain structure. In the literature, the grain size of a simplified square grain is usually defined as the side length of the square [1], [6], [7]. We thus define the size s_i of region i as $s_i = A_i^{0.5}$, i.e., as the side length of a square with equal area. The average grain size in the randomly-generated geometry can be forced to a desired value s_{av} by scaling the tessellated unit square with $ms_{\text{av}} / \sum_{i=1}^{m} s_i$. Such a scaling results into a calculation domain side length of approximately $L \approx m^{0.5} s_{\text{av}} = k s_{\text{av}}$ contrary to a periodic structure in which $L = m^{0.5} s_{\text{av}} = k s_{\text{av}}$ is exactly valid.

III. Results

A. Comparison of meshing approaches

We first consider a periodic grain structure similarly to [7], modeling 5 × 5 square grains of size $s_{\text{av}} = 17$ µm with a $d = 20$ nm boundary layer. In the ED case, ρ_{eff} is independent of the amplitude of V due to linearity. In the EMD case, an average flux density of amplitude of 0.1 T · (10 kHz / f)$^{0.5}$ is forced through Ω, so that q_{ind} in (4b) remains approximately the same as at 0.1 T and 10 kHz independently of the frequency. In both the ED and EMD cases, 21 logwise spaced frequencies in the range of $f \in$ [10 kHz, 1 GHz] are considered.

In Fig. 2, ρ_{eff} obtained with the structured and unstructured meshes and the TSM are compared. p_{cl} and q_{cap} cannot be similarly visualized, since they vary within several decades over the frequency range. Instead, Fig. 3 shows the ratios of p_{cl} and q_{cap} obtained with the unstructured mesh and the TSM with respect to those obtained with the structured mesh. Differences in q_{ind} are negligible. Both in Fig. 2 and Fig. 3, the TSM corresponds accurately to the results obtained with the structured mesh, and the results obtained with the unstructured mesh deviate slightly from the two.

Fig. 4 shows the current distributions in the EMD case obtained with each mesh and the TSM. At 10 kHz, the grains behave as insulated while at 100 MHz, the capacitive boundaries allow currents to flow over the whole domain. The TSM results correspond well to those obtained with the structured mesh. In the case of the unstructured mesh, slight oscillation is seen in the field lines at 100 MHz.

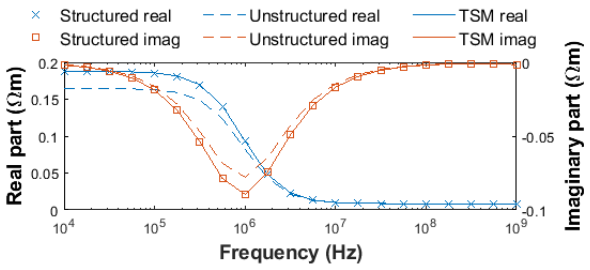

Fig. 2. ED formulation: Real and imaginary parts of the effective resistivity ρ_{eff} of a 5 × 5 grain structure modeled with the two meshes of Fig. 1 (a) and (b) and comparison to the TSM.

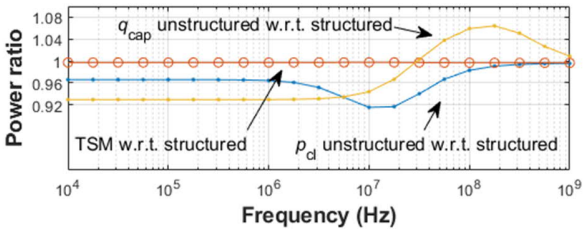

Fig. 3. EMD formulation: Ratios of eddy-current losses p_{cl} and capacitive power densities q_{cap} calculated with the unstructured mesh and TSM with respect to those calculated with the structured mesh in a 5 × 5 grain structure.

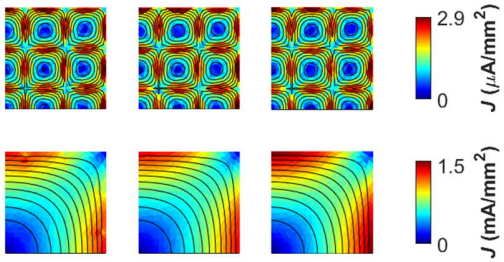

Fig. 4. EMD formulation: Current distributions $\|\boldsymbol{J} + j\omega\boldsymbol{D}\|$ in one quarter of the solution region at 10 kHz (top) and 100 MHz (bottom) obtained from the unstructured (left) and structured (center) meshes and the TSM (right).

B. Stochastic studies

We next apply the TSM to study the sensitivity of ρ_{eff}, p_{cl} and q_{cap} to the grain structure by creating 100 random geometries with $m = k^2 = 400$ grains, keeping the average grain size fixed to $s_{\text{av}} = 17$ µm. The results are compared to those obtained from a 20 × 20 periodic grain structure. The periodic geometry consists of 38599 nodes and 62158 triangular elements. The random geometries contain 38225 – 39401 nodes and 61349 – 63642 elements. Series calculation of the 100 × 21 = 2100 time-harmonic simulations for the random geometries took about 45 min in the ED case and 2.5 h in the EMD case using an in-house MATLAB-based solver on a laptop with a 2.8 GHz CPU and 32 GB RAM. The time includes the reading of the mesh files and the preprocessing required for doubling the boundary lines.

In Fig. 5, the real and imaginary parts of ρ_{eff} are plotted for each 100 geometries, highlighting the minimum and maximum

values. The variation range is rather small. Some deviations between the random and periodic geometries are observed in the real part at low frequencies and in the imaginary part at the dispersion region. The measurements digitized from [6] are provided as reference, and a good correspondence is observed.

Fig. 6 shows the ratios of p_{cl} and q_{cap} obtained from the random geometries with respect to those obtained from the periodic geometry. Quite large deviation is observed within the random geometries. It is notable that p_{cl} obtained from the random geometries is 20-50 % higher than the one obtained from the periodic geometry at $f < 10$ MHz. For q_{cap}, the difference is 20-40 %. The variation reduces at $f > 100$ MHz. For comparing the eddy-current losses against the results in [7], we scale them to a constant peak flux density of 10 mT, obtaining losses of 0.46 μJ/m^3, 48 μJ/m^3 and 95 mJ/m^3 at 10 kHz, 1 MHz and 100 MHz, respectively. The latter two values correspond roughly to those reported in Fig. 13 of [7], although the material parameters used in this paper are somewhat different.

IV. Discussion and Conclusion

The main advantage of the developed thin-shell model is its usability in the modeling of random geometries, in which the generation of structured meshes with good quality elements would be difficult. According to the results of Fig. 5, the random grain structures do not cause very much deviation in the effective resistivity. However, the results obtained from the random grain structures deviate slightly from those obtained from the periodic square grain structure with the same grain size.

According to Fig. 6, the random grain structure causes somewhat significant variations in the eddy-current losses and capacitive power densities below 10 MHz. The results also differ from those obtained from a periodic grain structure. However, at low frequencies, the eddy-current losses and capacitive power dissipation are very small and do not significantly contribute to the total losses or powers. The inductive power density was not affected by the grain structure.

Here the random geometries were scaled so that the average of the square roots of the individual grain areas was equal to the side length of the square grains in the periodic geometries, which was fixed to 17 μm based on [6]. In practice, the scaling could be chosen based on microscope images of real materials, and square grains with a suitably chosen side length could be used to approximate the behavior of the random geometries.

Acknowledgement

The Academy of Finland and the Emil Aaltonen foundation are acknowledged for financial support.

References

[1] F. Fiorillo et al., "Eddy-current losses in Mz-Zn ferrites," *IEEE Trans. Magn.*, Vol. 50, No. 1, Art. no. 6300109, 2014.

[2] F. Fiorillo, et al., "Approach to magnetic losses and their frequency dependence in Mn-Zn ferrites," *J. Appl. Phys.*, Vol. 89, Art. no. 122513, 2006.

[3] J. R. Shewchuck, "What Is a Good Linear Finite Element?- Interpolation , Conditioning, Anisotropy, and Quality Measures," In Proc. of the 11th International Meshing Roundtable, Ithaca, NY, USA, September 2002.

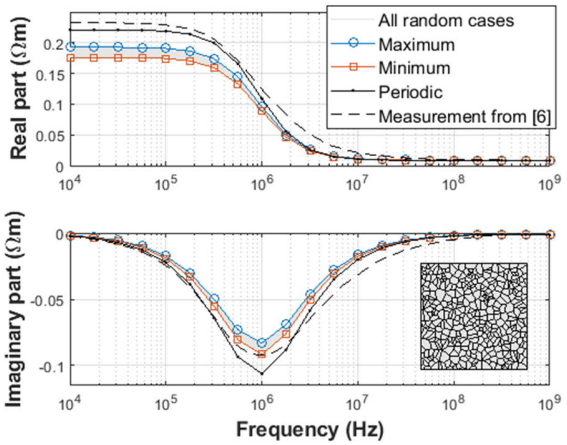

Fig. 5. ED formulation: Real and imaginary parts of the effective resistivity ρ_{eff} from 100 randomly generated geometries with compared to the ones obtained from a periodic geometry and the measurements of [6]. The inset shows an example of a random geometry with 400 grains.

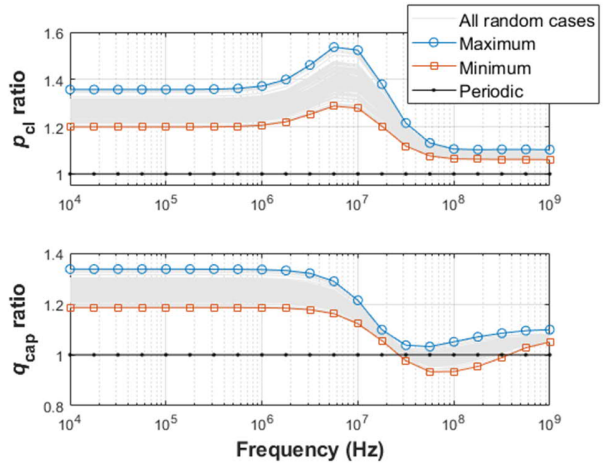

Fig. 6. EMD formulation: Ratios of eddy-current losses p_{cl} and capacitive power densities q_{cap} obtained from 100 random geometries to those obtained from a periodic grain structure.

[4] T. P. Todorova, A. Van den Bossche, V. C. Valchev, "A procedure for the extraction of intrinsic AC conductivity and dielectric constant of N87 Mn-Zn ferrite samples based on impedance measurements and equivalent electric circuit modeling," *IEEE Trans. Power Electron.*, Vol. 33, No. 12, pp. 10723-10735, 2018.

[5] M. Luo, D. Dujic, J. Allmeling, "Modeling Frequency Dependent Core Loss of Ferrite Materials using Permeance-Capacitance Analogy for System-Level Circuit Simulations," *IEEE Trans. Power Electron.* (in press).

[6] V. Loyau et al., "An analysis of Mn-Zn ferrite microstructure by impedance spectroscopy, scanning transmission electron microscopy and energy dispersion spectrometry characterizations," *J. Appl. Phys.*, Vol. 111, Art. no. 053928, 2012.

[7] O. Bottauscio, A. Manzin, "Comparison of multiscale models for eddy current computation in granular magnetic materials," *J. Comput. Phys.*, Vol. 253, pp. 1-17, 2013.

[8] K. Shimizu et al., "Loss Simulation by Finite-Element Magnetic Field Analysis Considering Dielectric Effect and Magnetic Hysteresis in EI-Shaped Mn-Zn Ferrite Cores," *IEEE Trans. Magn.*, Vol. 54, No. 11, Art. no. 7402705, 2018.

[9] Y. Ito, et al., "Effect of Magnetic Contact on Macroscopic Permeability of Soft Magnetic Composite," *IEEE Trans. Magn,*, Vol. 52, No. 3, 2016.

[10] E. Abenius, F. Edelvik, "Thin sheet modeling using shell elements in the finite-element time-domain method," *IEEE Trans. Antennas Propag.*, Vol. 54, No. 1, pp. 28-34, 2006.

[11] I. Benedetti, V. Gulizzi, "A grain-scale model for high-cycle fatigue degradation in polycrystalline materials," *Int. J. Fatigue*, Vol. 116, pp. 90-105, 2018.